

June 5, 1999

Functionally Independent Components of Early Event-Related Potentials in a Visual Spatial Attention Task

Scott Makeig* (1), Marissa Westerfield (2,5),
Jeanne Townsend (2,6), Tzyy-Ping Jung (4,5,6),
Eric Courchesne (2,6) and Terrence J. Sejnowski (3,4,5,6)

(1) Naval Health Research Center
P.O. Box 85122, San Diego CA 92186-5122
(619) 553-8414 office
(619) 587-0417 fax
scott@salk.edu

(2) Children's Hospital Research Center
San Diego CA 92123

(3) Howard Hughes Medical Institute
and
(4) Computational Neurobiology Laboratory
The Salk Institute for Biological Studies
10100 N. Torrey Pines Rd.
La Jolla, CA 92037

(5) Institute for Neural Computation
(6) University of California, San Diego
La Jolla, CA 92093

**To whom correspondence should be addressed.*

Abbreviated Title: **Components of Visual N1**

This report was supported by the Office of Naval Research, Department of the Navy (ONR.reimb.6429, S. Makeig), the Howard Hughes Medical Institute (T. Sejnowski), the National Institutes of Health (NINDS NS34155, J. Townsend and NIMH MH36840, E. Courchesne), and by the Swartz Foundation (T-P Jung and T. Sejnowski). The views expressed in this article are those of the authors and do not reflect the official policy or position of the Department of the Navy, Department of Defense, or the U.S. Government. Approved for public release, distribution unlimited.

Summary

Spatial visual attention modulates the first negative-going deflection in the human averaged event-related potential (ERP) in response to visual target and nontarget stimuli (the N1 complex). Here we demonstrate a decomposition of N1 into functionally independent subcomponents with functionally distinct relations to task and stimulus conditions. ERPs were collected from 20 subjects in response to visual target and nontarget stimuli presented at five attended and non-attended screen locations. Independent Component Analysis (ICA), a new method for blind source separation, was trained simultaneously on 500-msec grand average responses from all 25 stimulus/attention conditions and decomposed the nontarget N1 complexes into five spatially fixed, temporally independent and physiologically plausible components. Activity of an early, laterally symmetric component pair (N1a_R and N1a_L) was evoked by left and right visual field stimuli respectively. Component N1a_R peaked ~9 msec earlier than N1a_L. Central stimuli evoked both components with the same peak latency difference, producing a bilateral scalp distribution. Amplitudes of these components were not reliably augmented by spatial attention. Stimuli in the right visual field evoked activity in a spatiotemporally overlapping bilateral component (N1b) that peaked at around 180 msec and was strongly enhanced by attention. Stimuli presented at *unattended* locations evoked a fourth component (P2a) peaking near 240 msec. A fifth component (P3f) was evoked only by targets presented in either visual field. The distinct response patterns of these components across the array of stimulus and attention conditions suggest that they reflect activity in functionally independent brain systems involved in processing attended and unattended visuospatial events.

Key Words: *EEG, electroencephalogram, visual, event-related potential, ERP, spatial, attention, independent component analysis, ICA, N1, P2, P300, Interhemispheric transfer time*

INTRODUCTION

Early event-related potentials (ERPs) time locked to abrupt visual stimulus onsets are dominated by a vertex-negative potential deflection, often called N1, occurring from roughly 140 msec to 230 msec after visual stimulus onset. A prominent negative response peak with a similar latency, also called N1, but with a different scalp distribution, is evoked by auditory stimuli. However, neither the auditory nor the visual N1 responses are unitary (Naatanen & Picton 1987). In particular, visual N1 peak amplitude and latency are affected by both stimulus and task variables, including response cueing and attention to location or movement (Mangun & Hillyard 1991; O'Donnell *et al.* 1997; Kotchoubey *et al.* 1997; Valdes-Sosa *et al.* 1998).

An assumption implicit in most ERP research is that coherent neural activations producing ERP components occur in spatially-stable and restricted brain regions during information processing. This assumption is consistent with anatomical studies that separate visual cortex into discrete, interconnected regions, and with the spatially restricted activations typically observed in functional magnetic resonance imaging (fMRI) experiments. However, volume-conducted projections of spatially stable neural generators with overlapping time courses and scalp projections may produce the appearance of a single ERP peak having a moving scalp distribution. In this case, the separate projections may be called either components or subcomponents of the observed peak.

The scalp distribution of N1 typically changes smoothly during its time course. Because of this, it is suspected that the N1 arises from activity in multiple brain systems (Neville & Lawson 1987). However, decomposing the observed responses into subcomponents has not yet been accomplished. ERP components are usually identified with single response peaks in single channel waveforms. By this procedure, for example, Hillyard and Anllo-Vento (1998) and earlier researchers have identified an early and a late phase of the N1 complex. However, peak-based methods cannot be used to separate components if they do not produce separate peaks. In addition, spatial stationarity of the responses near a peak of interest is required to ensure that the peak is composed of only one spatially stable component.

Here, we apply Independent Component Analysis (ICA) (Bell & Sejnowski 1995; Makeig *et al.* 1996; Makeig *et al.* 1997; Makeig *et al.* 1999), a new approach to linear multivariate decomposition of multichannel data, to 31-channel recordings during a visual selective attention task (Townsend & Courchesne, 1994; Courchesne *et al.*, 1990). ICA decomposes ERP data into the sums of brief activations compatible with information processing in a small number of brain networks whose spatial projections to the scalp are fixed across time and task conditions. We hypothesized that data from this five-location selective-attention task might be better suited than simpler task paradigms for decomposing early visual components by ICA because this task involved a relatively large number of target and non-target response categories.

Most ERP studies of selective attention have analyzed responses to targets and to nontargets separately, since otherwise measures of early stimulus-related components of target responses might be confounded by overlapping early portions of later response-related components (e.g., Anllo-Vento & Hillyard 1996). The ICA method, however, may allow the time courses and scalp maps of these components to be separately identified in both target and nontarget responses simultaneously. For this reason, we applied ICA to data from all (25) target and nontarget conditions. Results suggest that visual evoked activity during the time course of the visual N1 in these experiments summed at least five functionally independent, spatially-stable components with distinct time courses, scalp maps and relationships to the stimulus and task conditions.

MATERIALS AND METHODS

[Figure 1 about here.]

Task design. Event-related brain potentials (ERPs) were recorded from subjects who attended to randomized sequences of filled round disks appearing briefly inside one of five empty squares which were constantly displayed 0.8 cm above a central fixation cross. The 1.6-cm square outlines were displayed on a black background at horizontal visual angles of 0° , $\pm 2.7^\circ$ and $\pm 5.5^\circ$ from fixation. During each 76-s block of trials, one of the five outlines was colored green and the other four blue. The green square marked the location to be attended. This location was counterbalanced across blocks. One hundred single stimuli (filled white circles) were displayed for 117 ms within one of the five empty squares in a pseudo-random sequence with inter-stimulus intervals (ISIs) of 250 to 1000 ms (in 4 equiprobable 250-ms steps).

Twenty right-handed volunteers (6 women, 14 men; ages 16 to 54 years) with normal or corrected to normal vision participated in the experiment. Subjects were instructed to maintain fixation on the central cross while responding only to stimuli (filled circles) presented in the green-colored (attended) square. Subjects were required to press a right-hand held thumb button as soon as possible following stimuli presented in the attended location. Thirty blocks of trials were collected from each subject, yielding 120 target and 480 nontarget trials at each location. Subjects were given 1-min breaks between blocks.

Evoked responses. EEG data were collected from 29 scalp electrodes mounted in a standard electrode cap (Electrocap, Inc.) at locations based on a modified International 10-20 System, and from two periocular electrodes placed below the right eye and at the left outer canthus. All electrodes were referenced to the right mastoid with input impedance less than 5k Ω . Data were sampled at 256 Hz or 512 Hz within an analog pass band of .01-50 Hz. All data were digitally converted to a 256 Hz sampling rate to minimize processing time. To further minimize line noise artifacts, responses were digitally low pass filtered below 40 Hz prior to analysis. After rejecting trials containing electrooculographic (EOG) potentials larger than 70 μ V, 500-msec (-100 ms to 400 ms) brain responses to stimuli presented at each location in each attention condition were averaged separately using the ERPSS software package (Hansen 1993), producing a total of 25 128-point ERPs for each subject. Responses to target stimuli were considered correct and averaged only when subjects responded between 150 and 1000 msec. No responses shorter than 200 msec were noted. Data averages studied in this report are available online at <http://www.cnl.salk.edu/~scott/20ssn1.txt.gz>.

Independent Component Analysis. The ICA algorithm we used in this study (Bell & Sejnowski 1995, 1996; Lee *et al.* 1999a) is an 'infomax' neural network (Linsker 1992; Nadal & Parga 1994) that uses stochastic gradient ascent to find a square 'unmixing' matrix that maximizes the joint entropy (Cover & Thomas 1991) of a nonlinearly transformed ensemble of zero-mean input vectors. Infomax ICA is one of a family of algorithms that exploit temporal independence to perform blind separation of linear mixtures of source signals. Recently, Lee *et al.* (1999a) have shown that these algorithms have a common information theoretic basis, differing chiefly in the form of source distribution, which may not be critical (Amari 1998). Logistic infomax can accurately decompose mixtures of component processes having symmetric or skewed distributions, even without using nonlinearities specifically tailored to them.

At the end of training, multiplying the input data by the output (or ‘unmixing’) weight matrix gives a data matrix whose rows, called the *component activations*, give the time course of relative strength or activity level of the respective independent components across conditions. ICA component activations are similar to the *factor weights* produced by spatial principal component analysis (PCA). The columns of the *inverse* of the weight matrix give the relative projection strengths of the respective components onto each of the scalp sensors. These may be interpolated to show the *scalp map* associated with each component. ICA scalp map weights are similar to spatial eigenvectors or *factor loadings* produced by spatial PCA.

Unlike components produced by PCA, however, component scalp maps returned by ICA are not constrained to be orthogonal and thus are free to accurately reflect the actual overlapping projections of functionally separate sources, if and when ICA successfully separates them. PCA is useful primarily for dimension reduction, but is less likely to separate data into functionally separate components. For example, Makeig *et al.* (1999) have shown that ICA, applied to these same response epochs (–100 to 900 ms) gave a decomposition of the Late Positive Complex (or P300) that was more tightly related to behavior, and better replicated between two subject subgroups than decompositions based on PCA with or without Varimax or Promax rotation.

The projection of the *i*th component onto the original data channels is given by the outer product of the *i*th column of the inverse weight matrix with the *i*th row of the component activation matrix, and is in the original units (e.g., μV). An overview of the assumptions of the ICA algorithm and their relation to ERP data is available elsewhere (Makeig *et al.* 1999). More information plus a collection of MATLAB routines for performing and visualizing the analysis are available via the World Wide Web (Makeig 1998).

Evoked response decomposition. In general, the independence assumption used by ICA is not known to hold exactly for actual ERP data. In this case very large components, including the late positive complex (LPC) in responses to target stimuli in these experiments, may possibly have a disproportionate influence on the decomposition of smaller components. For this reason, we selected an analysis time window ending 400 msec after stimulus onset. Trial decompositions of shorter time windows gave very similar results (though differing in some details, as discussed below), but did not include enough of the LPC onset to determine which LPC subcomponents contributed to the N1.

The logistic infomax ICA algorithm was applied to sets of 25 ERP averages (31 electrode channels, 128 time points) time locked from 100 ms before to 400 ms after onsets of target and nontarget stimuli presented at each of the 5 stimulus locations in the 5 spatial attention conditions. Decompositions were performed on grand averages of data from all 20 subjects using various time windows. Thus, a total of $5 \times 5 \times 31 = 775$ 500-msec ERP traces were analyzed simultaneously. ICA decomposition was performed using routines running under MATLAB 5.01 on a Dec Alpha 300 MHz processor (Makeig *et al.* 1997; Makeig *et al.* 1999). The learning batch size was 65. Initial learning rate started near 0.004, and was gradually reduced to 10^{-6} during 50-100 training iterations that required about 5 min of computer time. Results of the analysis were relatively insensitive to the exact choice of learning rate or batch size.

RESULTS

Averaged-evoked response decomposition

Although the appearance of the earliest recognizable visual evoked response peak, P1 (near 140 msec), was highly variable across the 25 response conditions, each contained a negative-going N1 component peaking at different scalp sites between 165 and 195 msec. The amplitude and duration of the N1 deflection varied considerably between scalp sites across stimulus and attention conditions. In all five target-response conditions, the N1 deflection was followed by P2 and N2 peaks, then a late positive complex (LPC, often called the P3 or P300) (Makeig *et al.* 1999).

[Figure 2[abcd] about here]

During the time course of the N1 response, the scalp topography of the responses changed continuously (Figure 2a, *scalp maps*), suggesting the presence of multiple overlapping components. The ICA decomposition of all 25 31-channel ERPs returned 31 components. Figure 2b shows the scalp maps of the six largest independent components. These had fixed scalp distributions and independent time patterns of activation across conditions. The largest two accounted for the early and middle phase of the LPC. Two others accounted for the late portion of the N1 and early portion of the P2 peaks, respectively. A third pair of components accounted for the early phase of the N1 in all conditions. One of these, which we labeled N1a_L, was activated by stimuli presented in the left visual field. The other, labeled N1a_R, was activated by right visual field stimuli. Stimuli presented in the central location, just above fixation, activated the left and right visual field response components together with near equal amplitudes. Components N1b and P2a peaked later than the N1a pair, whose scalp maps were nearly laterally symmetric. Still later and larger components P3f and P3b were evoked only by target stimuli.

Figure 2c illustrates a measure useful for visualizing the relation of component projections to the original data. The *envelope* of a multichannel data epoch may be defined as a pair of time series consisting respectively of the most positive and the most negative value in all or some data channels at each time point. For a given response epoch, the envelopes of the separate projections of each ICA component to the scalp electrodes may be defined similarly. Envelope plots can give useful indications of the latency, predominant polarity and amplitudes of temporally overlapping response and component features. The figure shows the grand mean target response at all 29 scalp channels (*blue traces*) above its data envelope (*black traces*).

Figure 2d (*black traces*) shows the envelopes of the grand mean responses to non-target stimuli presented in the far right, center and far left locations respectively, along with the envelopes of components N1a_R and N1a_L. The vertical dashed lines (at 162 msec) demonstrate that the activations of both components in response to central stimuli peak at the same latencies as in responses to lateral stimuli in which only one of the pair is active. At some time points, the data envelopes are smaller than the response envelopes. This occurred when the projections of other components (including N1b) had opposite signs at some scalp channels and canceled the N1a-component projections.

[Figure 3 about here]

To explore the patterns of activation of each of the components across conditions, the envelopes of each of the six component projections, in all 25 response conditions, were plotted in grid arrays (Figure 3). The top pair of grids show the activations of components N1a_L and N1a_R respectively. Within each grid, five columns (*left to right*) represent responses to stimuli presented at the respective

five locations, while the five rows (*top to bottom*) represent responses produced during attention to each of the same five locations. For maximum visibility, the envelope of the selected component projection is shown as a filled shape superimposed on the total response envelope. The left and right visual field response patterns of N1a_R and N1a_L are evident, as is their concurrent activation following centrally presented stimuli. There was no dramatic or consistent modulation of component amplitudes by attention. Although an interesting trend appeared in response to central stimuli (somewhat larger N1a_R amplitude when attention was to the left; somewhat smaller N1a_L amplitude in response to central targets), we did not yet test the between-subject reliability of these effects.

The complementary unilateral N1a_R and N1a_L response patterns are clearly seen in Figure 3. In response to leftmost stimuli, N1a_L accounted for nearly all of the early phase of the N1, while the N1a_R activation was very small and inconsistent. The opposite was true in responses to rightmost stimuli. Here, component N1a_R accounted for the early N1, and N1a_L had only a very small activation. Following central stimuli, however, both N1a_R and N1a_L were near-equally active.

Across all response conditions, the N1a_R peak occurred ~9 ms before the N1a_L peak (means across the 15 respective active conditions: 157.6 ± 2.7 msec versus 166.4 ± 3.7 msec). This latency difference was robust across conditions (by *t*-test, $p < 0.000001$). However, group means of the subject median reaction times to targets presented at the five locations had a different U-shaped character, with mean response time to central stimuli ~10 ms faster than responses to either leftmost or rightmost stimuli.

[Figure 4 about here]

To test the reliability of the latency difference across subjects, we applied the spatial filters for N1a_R and N1a_L to grand averages of responses to all left visual field (boxes 1 and 2) and right visual field (boxes 4 and 5) stimuli, respectively, from each of the twenty subjects. We then measured the latencies of the largest (frontal-negative) peak in the resulting activation waveforms between 145 and 185 msec. Results, illustrated in Figure 4 indicated a reliable tendency for N1a_R to peak earlier than N1a_L ($p < 0.02$ by *t*-test on the peak latency difference).

The middle pair of grids in Figure 3 shows the projections of components N1b and P2a. N1b was evoked nearly exclusively by stimuli presented at the midline and in right visual field. It was much larger following targets (*lower right diagonal*) than nontargets. There was no corresponding left-responding component; N1 in the left visual field conditions was nearly completely accounted for by N1a_L (*see upper-left grid*). Component P2a, on the other hand, was *smallest* following attended stimuli. It was evoked primarily by stimuli presented in non-attended locations, and particularly by non-attended midline stimuli. Responses to nontargets in the (Attend Mid-left / Present Far-left) and (Attend Mid-right / Present Far-right) conditions were also small, possibly reflecting a spatial generalization of response inhibition lateral to a left or right visual field attentional focus.

The bottom row of grids show the behavior of the first two of three components recently identified as contributing to the late positive complex (LPC) in these data (Makeig *et al.* 1999). Component P3f was evoked exclusively by stimuli presented in the attended location. P3f onset was near 160 msec, following the onsets of all three N1 components and near the N1a_R and N1a_L peaks. A much larger component, P3b (amplitude clipped at +2.5 μ V in the plot), was also evoked nearly exclusively by target stimuli. Onset of P3b (near 290 msec) followed the offset of the N1 deflection. Some small, disorganized P3b activation in response to nontarget stimuli may represent 'spillover' of this dominant component into other small and topographically similar data periods due to insufficient component independence in the ICA training data.

[Figure 5 about here]

Figure 5 shows results of bootstrap testing of the reliability of component N1a_R in single-subject decompositions. First, each subject's data (25 500-msec ERP averages) were decomposed using ICA. Next, the projections of the largest 16 independent components to 10 of the scalp channels (chosen at random to save computer resources) were compared using correlation to the projections of N1a_R to the same 10 channels in all 25 conditions. These correlations thus involved comparison of μV values at $25 \times 256 \times 10 = 64,000$ data points representing responses in all 25 stimulus/task conditions.

A second 500-msec time epoch (400 msec to 900 msec post stimulus) from the same epochs was used for comparison. Since dominant activity in N1 generators might be assumed to be absent in ERPs beginning more than 400 msec after a visual stimulus onset, these later data sub-epochs gave us an approximate or best available example of averages of spontaneous EEG epochs with the same number of sums as our early response epochs. Figure 5 (*thin starred traces*) shows the correlations between the projections of the best-fitting independent component (time courses times scalp maps) from the single-subject decomposition and the N1a_R in the grand-mean responses. (For the late-epoch components, the ordered absolute values of the correlations are shown). The two distributions are almost totally disjoint, reflecting the fact that N1-like activity was present in nearly every subject, and that ICA found at least one component of nearly every subject whose response map, time course and distribution across conditions resembled that of N1a_R. For 10 of the 20 subjects, the best correlation exceeded 0.4, a remarkable result considering that these correlations took into account both the scalp distributions and time courses of the entire 500-msec responses both within and across conditions.

The thick traces show the results of decomposing averages of all 25 early and late responses, respectively, from 200 random four-subject subgroups. Here the ensembles of best component correlations for the early and late epochs were even more disjoint, and the best-correlated early response component projection was correlated over 0.5 with the N1a_R projection for more than three-quarters of the four-subject averages. Applying the same process to averages of larger subject subgroups might be expected to produce components whose projections were closer and closer to N1a_R.

DISCUSSION*Functional Independence of ICA Components*

Although the N1 peak in these data contained only one broad positive peak at each scalp channel and condition (as in Figure 2a), ICA produced a robust and parsimonious decomposition of electrical activity during the N1 complex into at least five spatially fixed, temporally independent and partially overlapping components (N1a_L, N1a_R, N1b, P2a and P3f). The robustness of the decomposition, the relatively simple and distinct scalp distributions, and the selective modulation of the amplitudes of these components with the spatial location and the attended location suggest that they may correspond to functionally distinct brain systems. These results support the conclusions of earlier ERP researchers that the visual N1 response complex is comprised of more than one spatially stable component. However, before we can have confidence in the generality of these results, ICA decomposition of additional experiments using different spatial attention tasks is needed, as well as comparisons of single-subject decompositions of averages and single-trial data.

The problem of comparing group grand-mean response decompositions with ICA decompositions of single-subject responses is a difficult one. Grand-mean data sets have the unique

advantage that the strength of background EEG processes that are not time- and phase-locked by experimental events is reduced by a factor generally equal to the square root of the number of subjects. For experiments in which a relatively few trials are collected (e.g., target trials), this fact may be significant for ICA. Assuming that the number, timing and spatial projections of event-related brain processes (1) common to the group of subjects and (2) producing appreciable scalp potentials is relatively small, an ICA decomposition of grand-mean responses may have the best chance of recovering accurate evidence of the number, timing, and mean scalp projections of the processes. Single-subject averages, on the other hand, contain more remnants of background EEG processes, which are moreover superimposed by the averaging process, even if they actually occur in separate trials. The more processes summed in relatively brief evoked response epochs, the less chance that ICA can cleanly separate them, unless their independence is expressed across the ensemble of evoked responses representing multiple task and response conditions.

We have investigated three approaches to comparing single-subject responses using ICA. A simple and useful approach (cf. Figure 4) is to apply single component filters for independent components of the grand average to single-subject response data. Here the grand-mean components are used as measurement tools that combine multiple channels and/or time points in ways that are characteristic of the grand mean responses. This approach may compare favorably to separate measurements of response peaks at single scalp channels, when these peaks are composed of activity generated by different brain (or non-brain) sources. However, like single-channel peak measures, it may fail to take into account systematic differences in scalp projections and/or time courses in different subsets of the subjects.

A second approach is to apply separate decompositions to single-subject averages, or to averages of subgroups of subjects, as shown in Figure 5. Results of such comparisons, however, may be difficult to fit into a simple statistical model, since subjects may differ in the strengths, latencies, spectral character and scalp distributions of each of the components found in the grand mean decomposition. A third approach seeks to reduce the number of overlapping and non-independent EEG processes present in the data at each time point by simply decomposing ensembles of single-trials prior to any averaging. This approach shows great promise (Jung et al. 1999), but more work is necessary to thoroughly evaluate its usefulness.

P1 decomposition

In these experiments, the first positive visual evoked response peak, P1, appeared only in responses to stimuli presented at midline or, to a lesser extent, in the left visual field. The reason for this response variability is not known. Similar distributions were observed in averages of separate subject subgroups, so the P1 observed here is not an artifact of too few trials. Possibly, the location of the fixation point, slightly below the five stimulated locations, may account for the observed pattern. In the decomposition reported here, no single ICA component accounted for the P1. However, a single component accounting for most of the P1 activity did appear in an exploratory decomposition of these same data epochs using a narrower time window (-100 msec to 250 msec).

This difference between the two decompositions illustrates the statistical and exploratory nature of ICA decomposition given EEG data for which the ICA assumption of strict independence between source components may not precisely apply. Both ICA decompositions produced a set of multidimensional filters by which relatively independent variations in the data across time and conditions could be observed and measured. The usefulness of these decompositions depends on the degree to which they reveal or highlight functionally independent features in the data, and to the extent they generalize across experimental conditions.

N1a_R and N1a_L latency difference

The component scalp maps of the N1a_R and N1a_L were broadly distributed and bipolar (Figure 2b), compatible with the assumption that visual evoked response components originating in posterior visual cortex may propagate by volume conduction to EEG electrodes on all parts of the scalp. After their separation by ICA from three other overlapping response components and residual EEG, the activity of these two components were found to account for most or all early N1 activity in all 25 response conditions. In contrast to previous reports that central stimuli produce a bilateral N1 (Neville & Lawson 1987), ICA accounted for the bilateral N1 response to midline stimuli in these experiments as a sum of two lateralized components (N1a_R and N1a_L), each of whose 'receptive fields' included midline stimuli.

The stable tendency for component N1a_R to peak ~9 msec before N1a_L in these data, even in response to midline stimuli, replicates previous reports that right visual field stimuli tend to produce earlier N1 peaks at some scalp sites (Saron & Davidson 1989; Brown *et al.* 1994; Ipata *et al.* 1997). However, these authors measured this latency difference at individual electrode sites, and reported only a complex pattern of latency differences across the scalp. ICA, by contrast, gave nearly the same ~9-msec difference between the N1a_R and N1a_L peaks following either lateral or midline stimuli.

Previous reports have interpreted N1 latency differences observed at scalp sites ipsilateral and contralateral to the stimulated hemifield as a reflection of the callosal inter-hemispheric transfer time (IHTT). ICA, by contrast, modeled the N1 responses observed at each scalp site as weighted sums of the projected activity of at least five independent components. According to the ICA model, N1 peak latency at each scalp site depended on the relative strength and polarity of the projections of all five ICA components to that site, implying a complex relationship between single-electrode peak latencies and those of the underlying components, with little if any direct relationship to IHTT. The ~9 msec early-N1 latency difference provided by ICA, on the other hand, was independent of scalp channel, as well as being stable across conditions and subjects (Fig. 4). However, the origin and function of this difference are unknown.

N1a and attention

To a first approximation, N1a_R and N1a_L were not themselves modulated in any simple manner by visual spatial attention in these experiments (Fig. 3). The enlarged N1 peaks in responses to right visual-field attended stimuli were produced by substantial modulation of N1b by attention (see below); attended left-visual field stimuli in these experiments did not evoke an enlarged N1. It might prove revealing to fit the generators of N1a_R and N1a_L scalp distributions using multiple dipole or more general source models.

N1b and attention

In addition to the two early N1a components, ICA identified three later components whose activity began or peaked during the N1 complex under different conditions. Peak activations of these components were all strongly modulated by spatial attention. N1b, a left lateral-posterior negativity, responded to right visual field stimuli only, and much more strongly to targets. There was no homologous late-N1 deflection in the grand mean responses to left visual field stimuli (Figure 3) and therefore no corresponding independent component. The reason for this lateralized response difference is unknown. Several lines of evidence suggest that the right hemisphere is involved in attentional processing of information from both visual hemifields, while the left hemisphere directs attentional

responses to information in the right visual field only (Corbetta *et al.* 1993; Heilman *et al.* 1987; Mesulam 1981). Possibly, exclusive left-hemisphere attentional enhancement of attended right visual field stimuli is consistent with the asymmetry of the N1b, and right-hemisphere bilateral attentional control with the somewhat greater right-hemisphere involvement in later components P2a and P3b which were sensitive to attended locations in either hemifield.

P2a and inattention

P2a, a bilateral positivity largest at precentral and central posterior sites, was evoked primarily in response to *nontargets* in either hemifield. Its scalp map showed more right-central than left-central scalp activity. Components appearing only in response to stimuli presented in spatially *unattended* locations have not been previously reported, although it may have been present in previous selective attention responses (e.g., Figure 3 of Anllo-Vento & Hillyard 1996). For this and other components, ICA decomposition revealed a variety of systematic patterns of activation across response conditions that could easily have been missed even by expert observers. In particular, researchers looking for data features related to spatial attention might not expect to find that stimuli presented at *non-attended* locations in this experiment had a larger and topographically consistent early P2. Component P2a, however, exhibited this response profile, which was unique among the largest components, making it easy to identify.

The scalp distribution of P2a was anterior to the major target-evoked component, P3b (Makeig *et al.* 1999). Possibly, P2a might be involved in resetting cortex for further processing by adjusting short-term target-versus-nontarget expectancy. P3b, on the other hand, might reflect more widespread brain activity involved in resetting of both stimulus expectancy and response preparation following target events.

P3f and rapid responding

Component P3f had a bilateral frontoparietal scalp distribution, and was evoked only by target stimuli. Results shown in Figure 3 replicate our earlier observations, which was based on decomposition of 1-sec epochs (-100 msec to 900 msec) for ten of these subjects, that P3f onset in these experiments occurred near the peak of the N1 complex (Makeig *et al.* 1999). In faster responders among these subjects, P3f peak amplitude occurred very near the moment of the subcortical motor command (Makeig *et al.* 1999). The target selective nature of P3f, its frontoparietal topography, and its close association with response onsets in faster responders all suggest it may be associated with spatial orienting and motor response engagement. Its scalp distribution appears consistent with the bilateral frontoparietal pattern of hemodynamic activation reported recently by Corbetta *et al.* (1998) during both covert and overt shifts of attention from a central fixation point. Preliminary comparison of data from normal and clinical subjects in this task has suggested that the cerebellum may also play a role in the brain system P3f indexes (Westerfield *et al.* 1998).

In general, the physiological and cognitive functions of the brain systems generating visual evoked response components are unknown. By the time of their onset (all after 100 msec), information about the visual stimulus onset should already have propagated throughout visual cortex. This suggests that these components may be a reflection of later stages of visual processing rather than the earliest stages, which occur within the first 50 ms in primary visual cortex. One possibility is that N1 and subsequent ERP components (as well as still longer lasting event-related perturbations in the ongoing EEG spectrum) are involved in the integration of visual information across successive visual fixations, and/or in preparing cortex to process further visual information (Makeig 1993; Gilbert 1998).

Here we note that ICA can be seen as a very general information-based factor analytic method that may be usefully applied to analysis of multidimensional data in many contexts. Other promising ICA applications to brain data include analyses of functional magnetic resonance imaging (fMRI) (McKeown *et al.*, 1998), single-trial EEG analysis (Makeig *et al.*, 1998; Jung *et al.* 1999) and artifact removal (Jung *et al.* 1998), and optical recording data (Brown *et al.*, 1998).

Conclusions

These results demonstrate that ICA can decompose ERP data sets comprised of many scalp channels, stimulus types, and task conditions into temporally independent, spatially fixed, and physiologically plausible components without necessarily requiring the presence of multiple local response peaks. ICA decomposition provided a parsimonious model of these data that would have been difficult or impossible to build manually from separate consideration of all 775 single-channel waveforms that were simultaneously analyzed by ICA. The N1 components derived by ICA had distinct and simple-appearing scalp distributions. Each accounted for major features of some of the responses, and their patterns of activation covaried in unique but orderly ways with stimulus location and attended location. These findings are consistent with many anatomical and brain imaging studies showing that human cortex contains specialized systems that process various types of visual information, and that activity in many of these areas is enhanced by or requires spatial attention. The physiological origins and functions of these new ERP components deserve further analysis.

ACKNOWLEDGEMENTS

This report was supported by the Office of Naval Research, Department of the Navy (ONR.reimb.6429, S. Makeig), the Howard Hughes Medical Institute (T. Sejnowski), the National Institutes of Health (NINDS NS34155, J. Townsend; NIMH MH36840, E. Courchesne), and by the Swartz Foundation (T-P. Jung and T. Sejnowski). The views expressed in this article are those of the authors and do not reflect the official policy or position of the Department of the Navy, Department of Defense, or the U.S. Government. Approved for public release, distribution unlimited.

REFERENCES

- Amari, S. 1998 Natural gradient works efficiently in learning. *Neural Computation* 10, 251 276.
- Anllo-Vento, L., Hillyard, S. A. 1996 Selective attention to the color and direction of moving stimuli: electrophysiological correlates of hierarchical feature selection. *Percept. Psychophys.* 58, 191 206.
- Bell, A. J., Sejnowski, T. J. 1995 An information-maximization approach to blind separation and blind deconvolution. *Neural Computation* 7, 1129 1159.
- Bell, A. J., Sejnowski, T. J. 1996 Learning the higher-order structure of a natural sound. *Network: Computation in Neural Systems* 7, 261 270.
- Brown, G. D., Yamada, S., Luebben, H., Sejnowski, T. J. 1998 Spike sorting and artifact rejection by independent component analysis of optical recordings from tritonia. *Soc. Neurosci. Abst.* 24, 1670.
- Brown, W. S., Larson, E. B., Jeeves, M. A., 1994 Directional asymmetries in interhemispheric transmission time: evidence from visual evoked potentials. *Neuropsychologia* 32:, 439 448.
- Corbetta, M., Akbudak, E., Conturo, T. E., Snyder, A. Z., Ollinger, J. M., Drury, H. A., Linenweber, M. R., Petersen, S. E., Raichle, M. E., Van Essen, D. C., Shulman, G. L. 1998 A common network of functional areas for attention and eye movements. *Neuron* 21, 761 773.
- Corbetta, M., Miezin, F. M., Shulman, G. L., Petersen, S. 1993 A PET study of visuospatial attention. *J. Neurosci.* 13, 1202 1226.
- Courchesne, E., Akshoomoff, N. A., Townsend, J. 1990 Recent advances in autism. *Current Opinions in Pediatrics* 2, 685 693.
- Cover, T. M., Thomas, J. A. 1991 *Elements of Information Theory*. New York: John Wiley.
- Donchin, E. 1966 A multivariate approach to the analysis of average evoked potentials. *IEEE Trans. Biomed. Eng.* 13, 131 139.
- Gilbert, C. D. 1998 Adult cortical dynamics. *Physiological Reviews* 78, 467 485.
- Hansen, J. S. 1993 *Event-related Potential Software System*, La Jolla: Event-Related Potential Laboratory, University of California San Diego.
- Heilman, K. M., Watson, R. T., Valenstein, E., Goldberg, M. E. 1987 Attention: Behavioral and neural mechanisms. In *The Handbook of Physiology, Section 1: The Nervous System, Vol. V, Higher Functions of the Brain*. (ed. F. Plum, V. B. Mountcastle, S. T. Geiger). Bethesda, MD: American Physiological Association.
- Hillyard, S. A., Anllo-Vento, L. 1998 Event-related brain potentials in the study of visual selective attention. *Proc. Natl. Acad. Sci. USA* 95, 781 787.

Ipata, A., Girelli, M., Miniussi, C., Marzi, C. A. 1997 Interhemispheric transfer of visual information in humans: the role of different callosal channels. *Arch. Ital. Biol.* 135, 169 182.

Jung, T-P., Humphries, C., Lee, T-W., Makeig, S., McKeown, M., Iragui, V., Sejnowski, T. J. 1998 Extended ICA removes artifacts from electroencephalographic recordings. In: *Advances in Neural Information Processing Systems 10* (ed. M. M. Kearns, M. Jordan, S. Solla), pp. 894-900. Cambridge, MA: MIT Press.

Jung, T-P., Makeig, S., Westerfield, M., Townsend, J., Courchesne, E., Sejnowski, T. J. 1999 Analyzing and visualizing single-trial event-related potentials, *Advances in Neural Information Processing Systems 11*. (ed. M.S. Kearns, S.A.Solla, D.A. Cohn), pp. 894 900. Cambridge, MA: MIT Press.

Kotchoubey, B., Wascher, E., Verleger, R. 1997 Shifting attention between global features and small details: an event-related potential study. *Biol. Psychol.* 46, 25 50.

Lee, T-W., Girolami, M., Bell, A. J., Sejnowski, T. J. 1999a A unifying framework for independent component analysis. *Int. J. Math. Computer Models*.

Lee, T-W., Girolami, M., Sejnowski, T. J. 1999b Independent component analysis using an extended infomax algorithm for mixed sub-gaussian and super-gaussian sources. *Neural Computation* 11, 417-441

Linsker, R. 1992 Local synaptic learning rules suffice to maximise mutual information in a linear network. *Neural Computation* 4, 691 702.

McKeown, M. J., Makeig, S., Brown, G. G., Jung, T-P., Kindermann, S. S., Bell, A. J., Sejnowski, T. J. 1998b Analysis of fMRI data by blind separation into independent spatial components. *Human Brain Mapping* 6, 160 188.

Makeig, S. 1993 Event-related dynamics of the EEG spectrum and effects of exposure to tones. *Electroencephalogr. clin. Neurophysiol.* 86, 283 293.

Makeig, S. *et al.* 1998 *MATLAB toolbox for electrophysiological data analysis*. WWW Site, Computational Neurobiology Laboratory, Salk Institute, La Jolla CA, <http://www.cnl.salk.edu/~scott/ica.html> [World Wide Web Publication].

Makeig, S., Bell, A. J., Jung, T-P., Sejnowski, T. J. 1996 Independent component analysis of electroencephalographic data. In: *Advances in Neural Information Processing Systems 8* (ed. D. Touretzky, M. Mozer, M. Hasselmo), pp. 145 151. Cambridge, MA: MIT Press.

Makeig, S., Jung, T-P., Ghahremani, D., Bell, A. J., Sejnowski, T. J. 1997 Blind separation of auditory event-related brain responses into independent components. *Proc. Natl. Acad. Sci. USA* 94, 10979 10984.

Makeig, S., Jung, T-P., Sejnowski, T. J. 1998 Multiple coherent oscillatory components of human electroencephalogram (EEG) are differentially modulated by cognitive events. *Soc. Neurosci. Abst.*

Makeig, S., Westerfield, M., Jung, T-P., Covington, J., Townsend, J., Sejnowski, T. J., Courchesne, E. 1999 Independent components of the late positive event-related potential in a visual spatial attention task, *J. Neurosci.* 19, 2665 2680.

Mangun, G. R., Hillyard, S. A. 1991 Modulations of sensory-evoked brain potentials indicate changes in perceptual processing during visual-spatial priming. *J. Exp. Psychol. Hum. Percept. Perform.* 17, 1057 1074.

Mesulam, M. M. 1981 A cortical network for directed attention and unilateral neglect. *Ann. Neurol.* 10, 309 325.

Nadal, J-P., Parga, N. 1994 Non-linear neurons in the low noise limit: a factorial code maximises information transfer. *Network* 5, 565 581.

Naatanen, R., Picton, T. 1987 The N1 wave of the human electric and magnetic response to sound: a review and an analysis of the component structure. *Psychophysiology* 24, 375 425.

Neville, H. J., Lawson, D. 1987 Attention to central and peripheral visual space in a movement detection task: an event-related potential and behavioral study. I. Normal hearing adults. *Brain Res.* 405, 253 267.

O'Donnell, B. F., Swearer, J. M., Smith, L. T., Hokama, H., McCarley, R. W. 1997 A topographic study of ERPs elicited by visual feature discrimination. *Brain Topogr.* 10, 133 143.

Saron, C. D., Davidson, R. J. 1989 Visual evoked potential measures of interhemispheric transfer time in humans. *Behav. Neurosci.* 103, 1115 1138.

Townsend, J., Courchesne, E. 1994 Parietal damage and narrow "spotlight" spatial attention. *J. Cogn. Neurosci.* 6, 220 232.

Valdes-Sosa, M. Bobes, M. A., Rodriguez, V., Pinilla, T. 1998 Switching attention without shifting the spotlight object-based attentional modulation of brain potentials. *J. Cogn. Neurosci.* 10, 137 151.

Westerfield, M., Townsend, J., Makeig, S., Jung, T-P., Sejnowski, T. J., Courchesne, E. 1998 Independent components of the late positive event-related potential in a visual spatial attention task: normal and clinical subject differences, *Soc. Neurosci. Abst.* 24:507.

FIGURE CAPTIONS

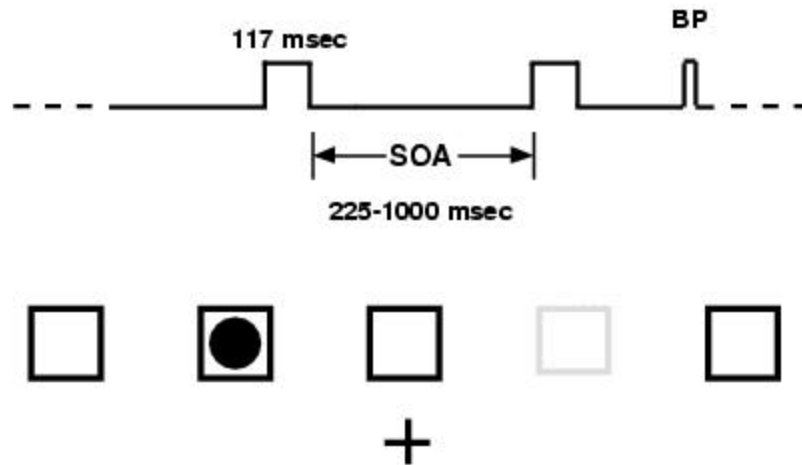


Figure 1. Schematic time line and stimulus display for the experiment. Subjects fixated the screen center (*cross, lower row*), while five boxes were continuously displayed above the fixation point. During each 76-sec block of trials, one of the boxes was colored differently from the others, indicating that it was the attended stimulus location for that block. Visual stimuli (*single solid disks, duration 117 msec*) were briefly displayed in boxes 1 (*leftmost*) to 5 (*rightmost*) in pseudo-random order at inter-stimulus intervals of 225 msec to 1000 msec. Subjects were asked to press a right thumb button as soon as possible whenever a disk was presented in the attended location.

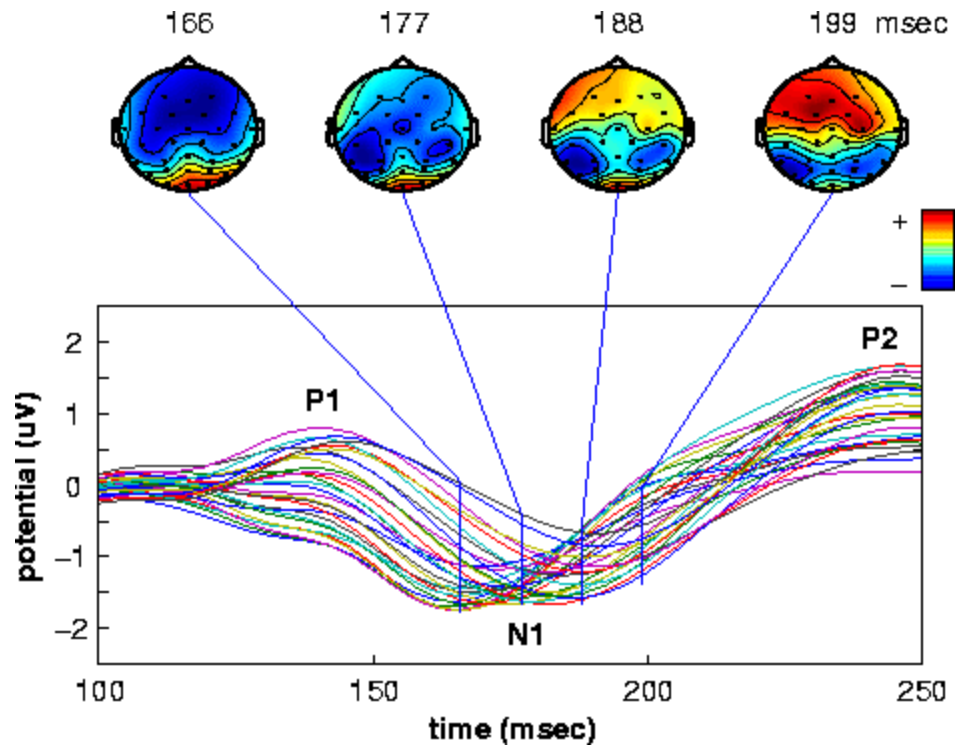


Figure 2a. The grand mean response for all 20 nontarget conditions and 20 subjects. Responses at all 29 scalp channels are shown on the same baseline. Note that N1 component peak latency differs at each electrode site. The scalp maps illustrate the continuously shifting potential distribution through the N1 peak. The maps have been scaled individually to their minimum and maximum values to highlight shifts in the scalp distribution of the response.

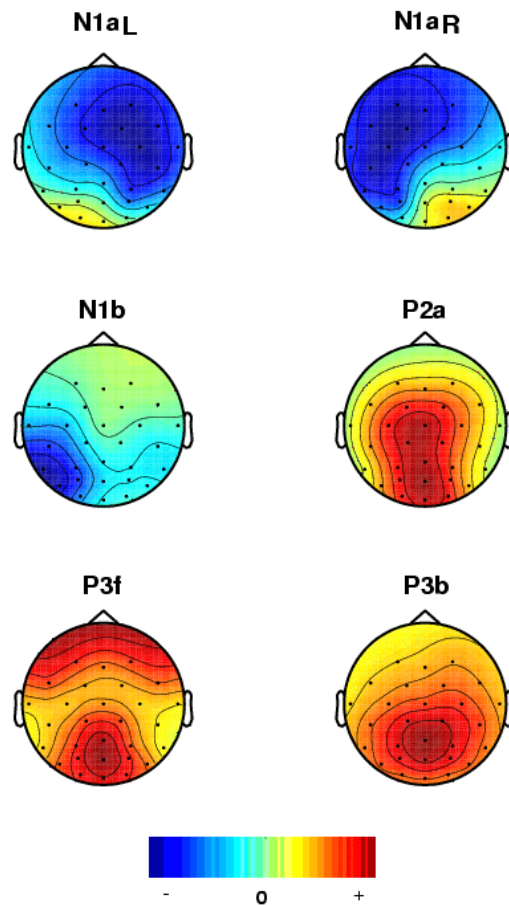


Figure 2b. Scalp maps of the largest six independent components, individually scaled (*green represents zero weight*). Relative locations of the electrodes are shown by small dots. Color polarities are chosen to represent the signs at their time point of maximum projection (*with red positive, blue negative with respect to the reference*). Note the bilateral near-symmetry of the two early-N1 components (*top row*).

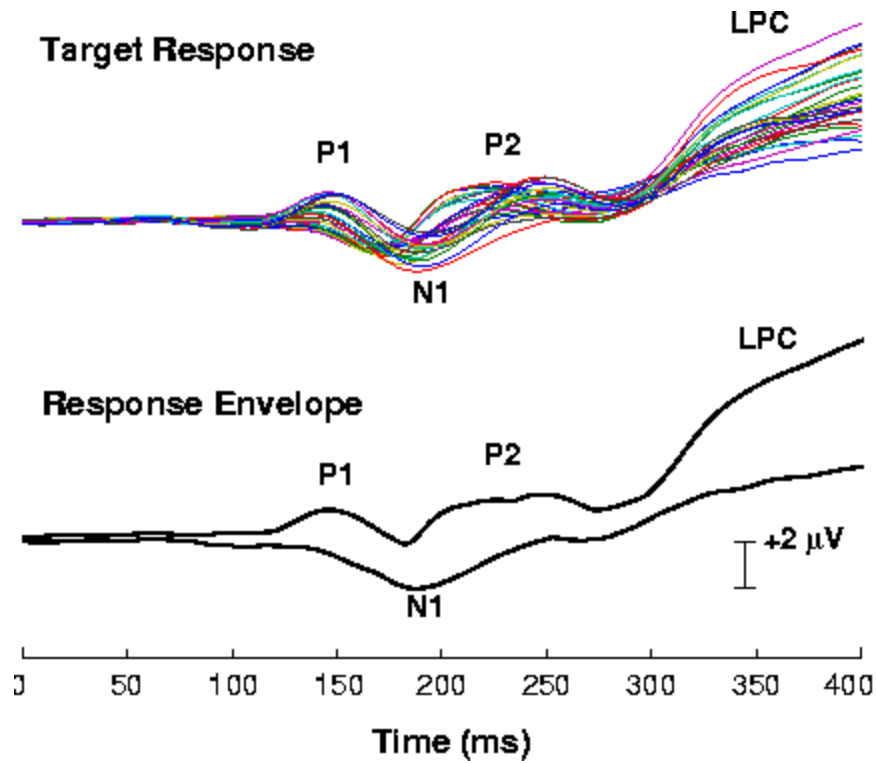


Figure 2c. The upper (*blue*) traces show the grand mean target response averaged across all 20 subjects and 5 target conditions at the 29 scalp channels. The time series defined by the most positive and most negative potential values across all channels at each time point may be termed the 'envelope' of the data, as shown in the lower panel (*black traces*). Conventional peak labels are shown.

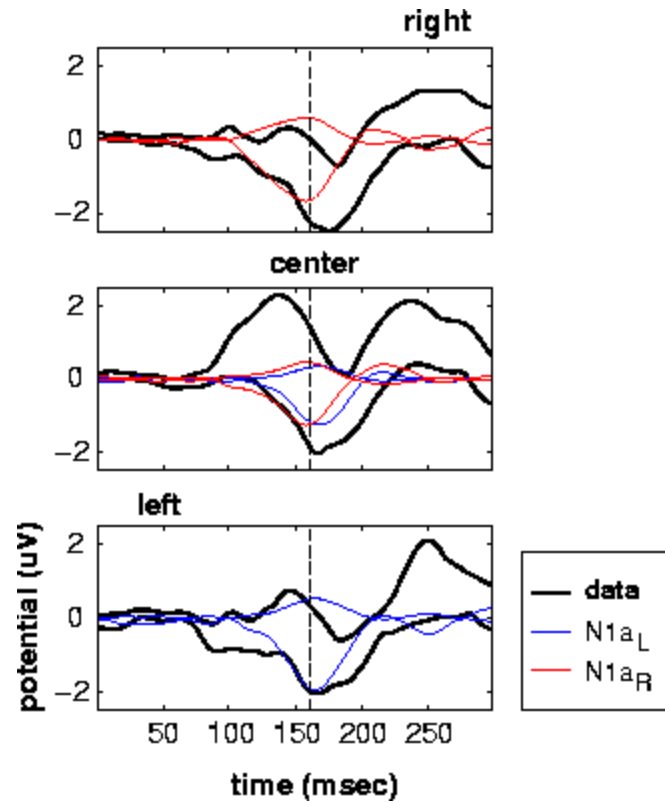


Figure 2d. Envelopes of independent components N1a_L and N1a_R in the grand mean responses to non-target stimuli presented at far right, central, and far left locations respectively. The vertical dashed lines mark 162 msec. Note the stable component peak latencies across conditions, and their ~9 msec difference. Envelopes computed across 29 scalp channels.

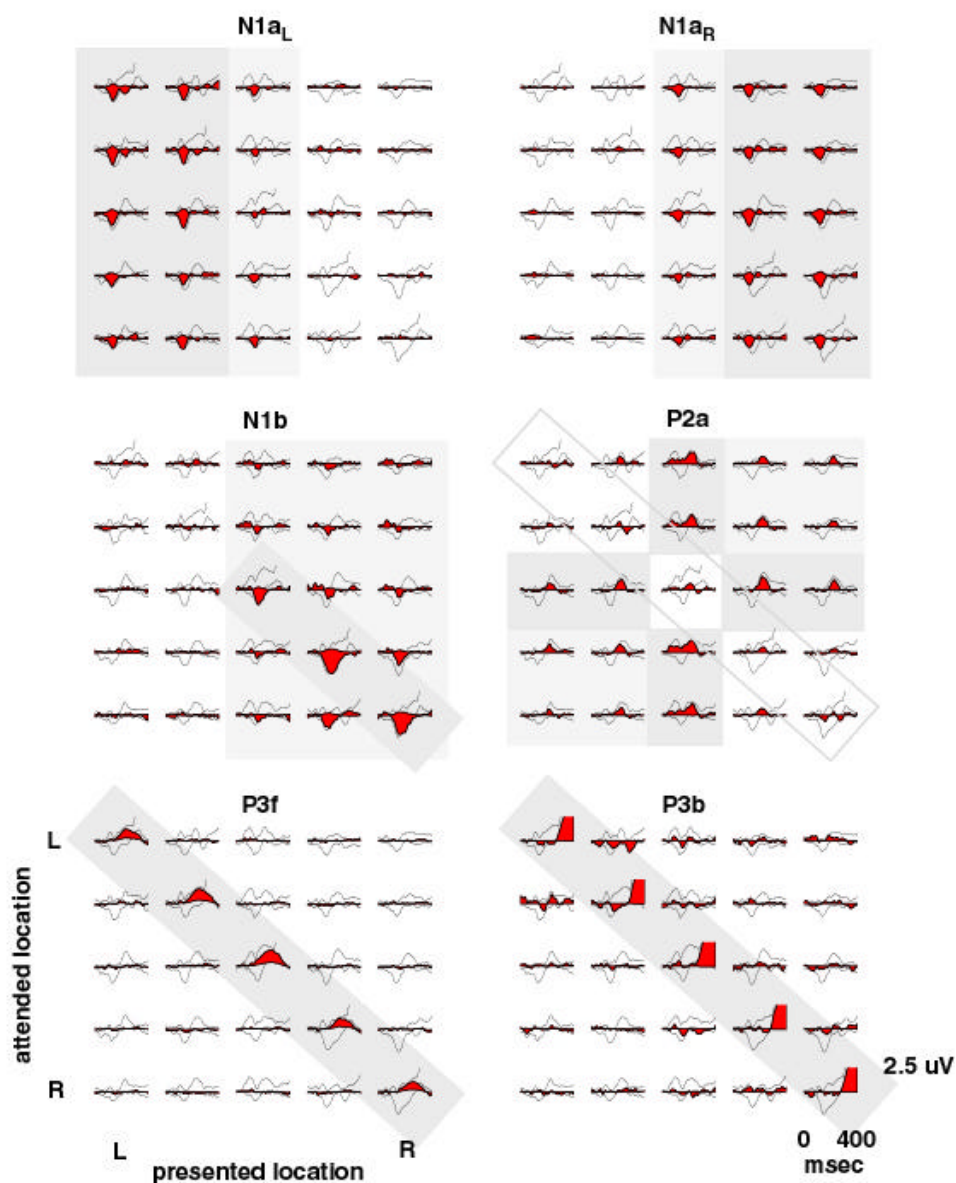


Figure 3. Envelopes of the six largest independent components (*black outline, filled with red, from all 29 scalp and 2 EOG channels*) (cf. Fig. 2b above), superimposed on the mean response envelopes for all 25 Presented/Attended Location conditions. Note the systematic differences between the sets of conditions in which the different components are active: N1a_L and N1a_R (*top row*) are evoked by left and right visual field stimuli, but do not appear to depend in any simple way on the attended location. Both also respond to midline stimuli. N1b (*center left*) responds to right visual field stimuli. Its amplitude is enhanced both in attended locations and to a lesser extent in nearby right visual field locations (*locations (4,5) and (5,4)*). P2a, by contrast (*middle right*), has little or no response to targets (*diagonal traces*). Its amplitude is generally largest to nontarget midline stimuli. Components P3f (*lower left*) and P3b (*lower right, amplitude clipped*) account for overlapping early and middle portions of the late positive complex (Makeig *et al.*, 1999) in responses to target stimuli presented at attended locations.

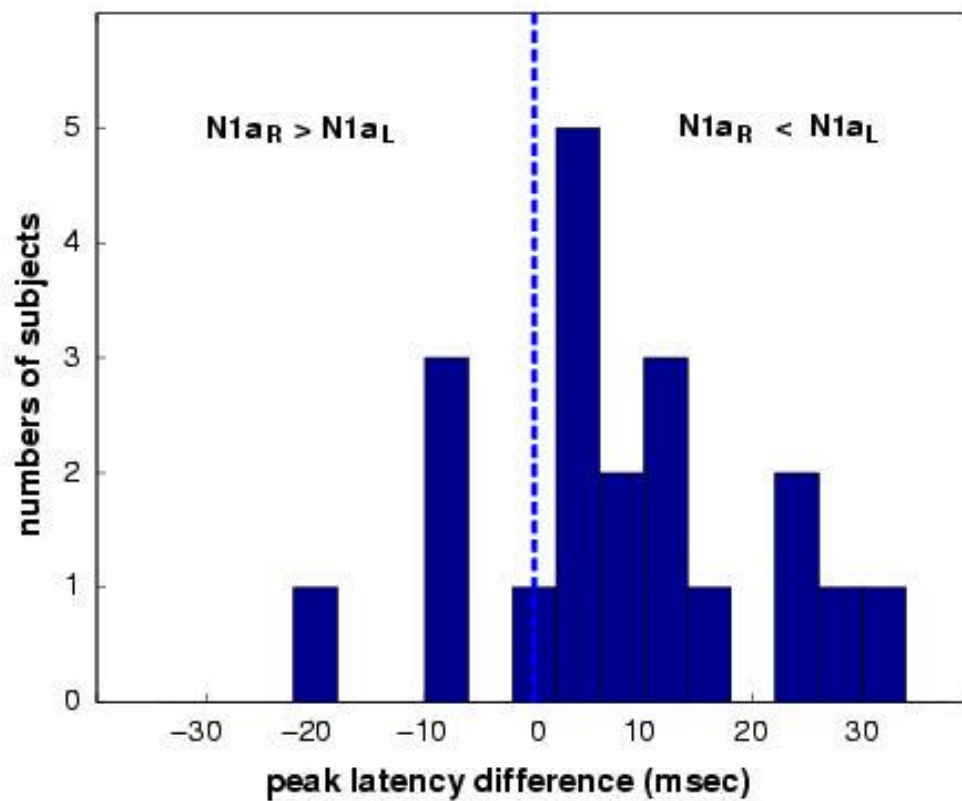


Figure 4. Histogram of peak latency differences between components $N1a_R$ and $N1a_L$ in single subjects. Differences computed by applying the spatial filters for these two components derived from the grand averages to the 20 single-subject mean responses to left visual field (*box 1 or 2*) and right visual field (*box 4 or 5*) stimuli respectively. Results (significant by *t*-test, $p < 0.02$) compare well with the ~ 9 msec ($N1a_R - N1a_L$) latency difference found in the grand average decomposition (Fig. 2d).

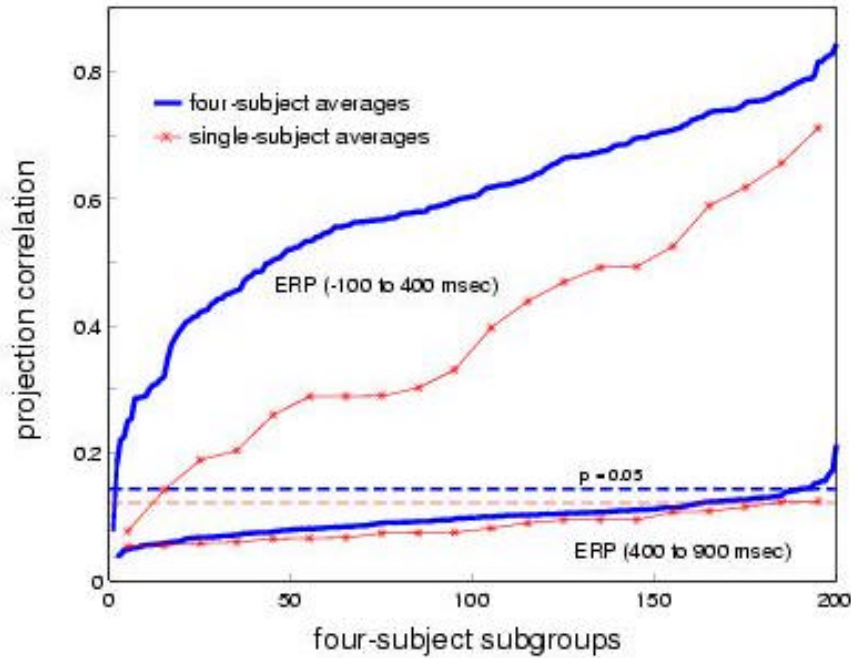


Figure 5. Bootstrap analysis of variability in ICA decompositions from single subjects and subject subgroups. Plot shows rank-ordered correlation coefficients between the time course in all 25 conditions of component N1a_R (from the grand average decomposition) and (*thin traces*) the time course of the most highly-correlated independent component derived from separate training on each of the 20 subjects' data, or (*thick lines*) on averages of data from 200 randomly-selected subgroups of 4 subjects. The top two traces show correlations between ERPs in the time range -100 msec to 400 msec. As a control, data from a later portion of the same response epochs (400 msec to 900 msec post-stimulus onset) were used to derive ICA components, and the resulting component projections were correlated with the same grand-mean N1a_R projection (*lower traces*) Note that nearly all the control correlations fall below the dashed lines that give the p=0.05 confidence levels in the single-subject and subject subgroup control data results